PROTEINS: Structure, Function, and Genetics 20:4–14 (1994)

RESEARCH ARTICLES

Protein Stability Parameters Measured by Hydrogen Exchange

Yawen Bai, John S. Milne, Leland Mayne, and S. Walter Englander
The Johnson Research Foundation, Department of Biochemistry and Biophysics, University of Pennsylvania School of Medicine, Philadelphia, Pennsylvania 19104-6059

ABSTRACT **The hydrogen exchange (HX) rates of the slowest peptide group NH hydrogens in oxidized cytochrome c (equine) are controlled by the transient global unfolding equilibrium. These rates can be measured by one-dimensional nuclear magnetic resonance and used to determine the thermodynamic parameters of global unfolding at mild solution conditions well below the melting transition. The free energy for global unfolding measured by hydrogen exchange can differ from values found by standard denaturation methods, most notably due to the slow cis-trans isomerization of the prolyl peptide bond. This difference can be quantitatively calculated from basic principles. Even with these corrections, HX experiments at low denaturant concentration measure a free energy of protein stability that rises above the usual linear extrapolation from denaturation data, as predicted by the denaturant binding model of Tanford.** © 1994 Wiley-Liss, Inc.

Key words: thermodynamic parameters, cytochrome c, protein folding

INTRODUCTION

To understand the factors that determine protein structural stability and function, one wants to measure stability and changes in stability due to temperature, solvent conditions, functional state, amino acid substitutions, and other modifications in terms of real thermodynamic parameters. At this time the measurement of thermodynamic stability parameters depends on carrying a protein through its global unfolding transition where K_{unf}, the equilibrium constant for unfolding, can be measured. One can then attempt to extrapolate these stability measurements to obtain parameters at milder solution conditions.

Measurements of K_{unf} through the unfolding transition are commonly made by spectroscopic methods or calorimetric heat absorption. These approaches are not without problems. Denaturant melting experiments provide data only over a limited range, often have sloping baselines, and require long extrapolations with uncertain degree of curvature.[1–3] Analysis of calorimetric data can be impaired by baselines that slope or even curve, and by high melting temperatures, and proteins may exhibit irreversibility when heat denatured at the concentrations required.[4] Horse cytochrome c (cyt c), for example, tends to aggregate when melted at pH values above 5.

In recent work, Mayo and Baldwin[5] studied the dependence of ribonuclease hydrogen exchange (HX) on low concentrations of guanidinium chloride (GdmCl) and suggested that exchange of the slow NHs may be determined by a novel whole-molecule mechanism, termed global unlocking, acting in tandem with a series of more limited fluctuations. Following their lead, we initiated similar studies on cyt c. HX measurements over a wider range of GdmCl concentrations and temperature now point to a somewhat simpler conclusion. GdmCl and temperature act by promoting the transient global unfolding reaction itself, which in turn determines the HX behavior of the slowest exchanging hydrogens. This is possible because protein molecules cycle through the globally unfolded state, as required by the Boltzmann distribution, even under mild solution conditions. Thus the very slow HX behavior can be exploited to measure global protein unfolding and its response to experimental variables at conditions well below the melting transition. Available evidence suggests that this capability is fairly general.

THEORETICAL BACKGROUND

This section considers the relationships among protein hydrogen exchange, transient unfolding,

Received February 4, 1994; revision accepted May 5, 1994.
Address reprint requests to Walter Englander, The Johnson Research Foundation, Dept. of Biochemistry and Biophysics, University of Pennsylvania School of Medicine, Philadelphia, PA 19104-6059.

and structural stability, and shows how HX measurements taken as a function of denaturant concentration and of temperature are able to access thermodynamic parameters.

Thermodynamic Parameters From HX Data

The exchange of protein hydrogens that are slowed by involvement in structure depends on some structural opening step, as in Eq. 1.

$$\text{closed} \underset{k_{cl}}{\overset{k_{op}}{\rightleftarrows}} \text{open} \xrightarrow{k_{rc}} \text{exchange: } K_{op} = k_{op}/k_{cl} \quad (1)$$

In the steady state, this reaction sequence produces HX rates given by Eq. 2.

$$k_{ex} = k_{op}k_{rc}/(k_{op} + k_{cl} + k_{rc}) \quad (2)$$

At the so-called EX1 limit,[6] where $k_{cl} << k_{rc}$, Eq. 2 leads to the HX rate in Eq. 3.

$$k_{ex} = k_{op} \quad (3)$$

Eq. 4 gives the HX rate at the EX2 limit, where $k_{cl} >> k_{rc}$.

$$k_{ex} = (k_{op}/k_{cl})k_{rc} = K_{op}k_{rc} \quad (4)$$

These equations assume that structure is stable, so that $K_{op} << 1$. K_{op} is then essentially equal to the fraction of time the restraining structure is open [fraction open = $K_{op}/(K_{op} + 1)$]. We assume EX2 behavior here, and will describe experimental tests of this assumption. In the EX2 limit the measurement of an HX rate provides the free energy for the underlying structural opening reaction, according to Eq. 5.

$$\Delta G_{HX} = -RT \ln K_{op} = -RT \ln(k_{ex}/k_{rc}) \quad (5)$$

Since values for k_{rc}, the HX rate for NHs in a random chain polypeptide, are known,[7,8] the measurement of k_{ex} leads to K_{op} (Eq. 4), and therefore to ΔG_{HX}. These issues have been multiply recounted before,[9] from the point of view of a supposed dependence of H-exchange on the opening of individual H-bonds,[6,10] on the cooperative unfolding of small structural segments[11,12] and on global whole molecule unfolding.[13]

We want to consider the case in which structural opening reactions can be manipulated by temperature and denaturants, and in which significant rate contributions for a given NH may come from both local (l) and global (g) opening events. In this case, Eqs. 6 and 7 will come into play.

$$k_{ex} = k_{ex}(l) + k_{ex}(g) = [K_{op}(l) + K_{op}(g)]k_{rc} \quad (6)$$

$$\Delta G_{HX} = -RT \ln[K_{op}(l) + K_{op}(g)] = -RT \ln K_{op,eff} \quad (7)$$

In general, limited structural fluctuations will have low sensitivity to temperature and denaturants. Global unfolding will be more sensitive. Let us consider the consequences for protein HX behavior.

Structural Free Energy From Denaturant Studies

Figure 1a uses hypothetical data for the unfolding of a protein with denaturant to illustrate the analysis commonly used to measure structural stability.[3] Measurement of any structure-sensitive parameter through an unfolding transition can provide the equilibrium unfolding constant (K_{unf} (Den) = [Unf]/[Nat]), and from this the free energy for unfolding ($\Delta G(Den) = -RT \ln K_{unf}$) as a function of denaturant concentration in the immediate transition region. To obtain the stabilization free energy at zero denaturant concentration [$\Delta G(0)$], one usually extrapolates from the data as shown in Figure 1a (solid line). This procedure assumes a linear dependence on denaturant concentration as in Eq. 8.

$$\Delta G_{unf}(Den) = \Delta G(0) - m[Den] \quad (8)$$

The slope, m, relates to the exposure of new denaturant binding surface when the protein unfolds.[3]

Due to the long extrapolation from a limited data range (Fig. 1a), the accuracy of $\Delta G(0)$ obtained in this way is exceedingly sensitive to the detailed accuracy of the data, including necessary corrections for baseline non-linearity above and below the transition.[3] Further, according to the denaturant binding model of Tanford,[1,2] which considers the differential binding of denaturant to a limited number of sites, the extrapolation may properly curve upward, as suggested by the dashed line in Figure 1a. This behavior can be approximated as in Eq. 9.

$$\Delta G(Den) = \Delta G(0) - \Delta nRT \ln (1 + K_b[Den]) \quad (9)$$

Here Δn is the number of additional denaturant binding sites, with averaged binding constant K_b, that are exposed when the protein unfolds.

Two previous attempts to test these models by calorimetric measurements reached opposite conclusions,[14,15] due in part to the difficulty of obtaining an accurate post-transition baseline as temperature approaches 100°C. Ideally one would like to obtain a direct measurement of $\Delta G(Den)$ in the range of low denaturant concentration where the linear and denaturant binding models diverge (Fig. 1a). This would more precisely determine the $\Delta G(0)$ value as well as distinguish different models for denaturant processes.

Given the relationships indicated in Eq. 5, HX measurements in the range of low denaturant concentration may provide this information. In general, the HX rate for any given NH depends on the fraction of time its blocking structure is open, i.e., on the sum of its local (l) and global (g) openings, as in Eq. 6. The summed fraction of time open, $K_{op,eff}$ (Eq. 7),

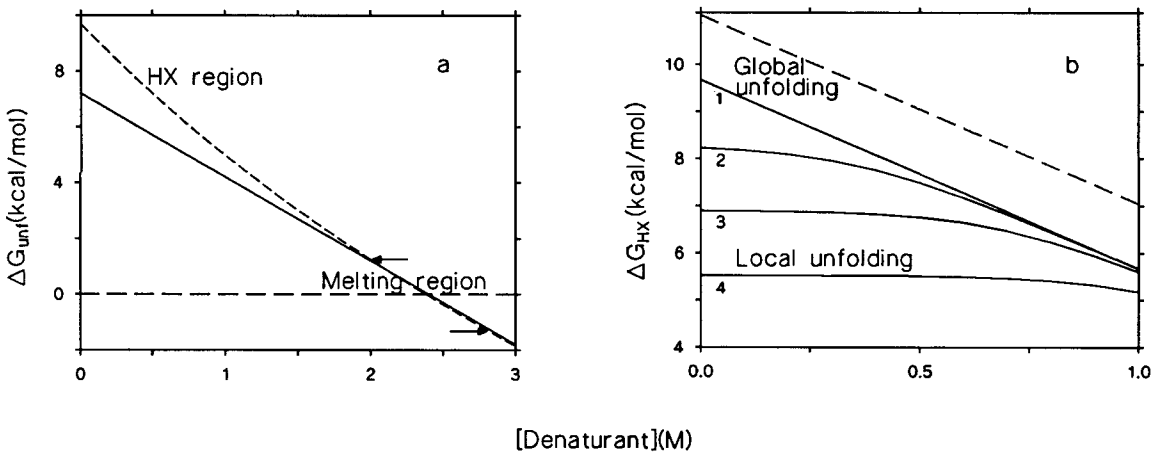

Fig. 1. Illustrative curves for the dependence of unfolding free energy on denaturant concentration. **a:** Linear extrapolation of the free energy for global unfolding measured in the transition region (Eq. 8, using hypothetical parameters). The rising, dashed curve is suggested by the denaturant binding model (Eq. 9). **b:** Relationship between the free energy measured by HX of a very slowly exchanging NH (1) that depends on $K_{op}(g)$ and some faster NHs (2–4) with different $K_{op}(1)$ (Eq. 7). The upper dashed curve represents an NH that experiences some residual HX blocking in the $K_{op}(g)$ state, so that it exchanges from a still higher energy state, as expressed by B(g) = 0.1.

can be written as in Eq. 10 to include the denaturant dependence in the linear approximation (Eq. 8).

$$K_{op,eff} = K(l)_{op} + K(g,0)_{op}\exp(m[Den]/RT) \quad (10)$$

Eq. 10 assumes that local openings are insensitive to denaturant (m = 0) and takes the final term from Eq. 8, where K(g,0) represents K(Den) for global opening at zero denaturant. Eq. 10 together with Eq. 6 describes the dependence of HX rate on denaturant concentration in the linear approximation.

Figure 1b simulates behavior that might be expected for the exchange of various NHs. The simulation was prepared using reasonable values for the local and global parameters in Eq. 10, together with Eq. 7. The uppermost solid curve in Figure 1b represents NHs that can exchange only by way of a global unfolding, with $\Delta G(g)$ = 9.7 kcal/mol and m = 4 kcal/mol/(molar denaturant). The simulation assumes that m for the global unfolding is constant over the small denaturant range and low denaturant concentration shown. The lower lying curves in Figure 1b represent faster NHs that exchange by way of smaller opening reactions, with $\Delta G(l)$ less than $\Delta G(g)$. We assume $m \approx 0$ for these local openings, since little new surface will be exposed in small fluctuations. Figure 1b shows that global unfolding makes no significant contribution to the faster NHs at low denaturant. As denaturant concentration increases, the global unfolding equilibrium is selectively promoted because its m value is large, and so it progressively overtakes the faster exchanging NHs.

The HX analysis described assumes that HX rate in transiently open forms is equal to k_{rc}, the rate calibrated in random chain polypeptides.[7,8] If residual blocking structure is present in unfolded forms, HX results may be able to detect this. This possibility can be accommodated in Eqs. 6 and 7 by multiplying $K(l)_{op}$ and/or $K(g)_{op}$ by factors less than unity, e.g., by B(l) and B(g), respectively. The dashed line in Figure 1b indicates the effect of a factor B(g) = 0.1, so that HX rate of the proton in some otherwise measurable globally unfolded form is still slowed tenfold (see also refs. 13, 24–26).

Energy Parameters From Temperature Studies

The general dependence of protein unfolding free energy on temperature is shown in Figure 2a. Equation 11 describes this behavior.[4]

$$\Delta G(T) = \Delta H_m - T\Delta S_m + \Delta Cp[(T - T_m) - T \ln(T/T_m)] \quad (11)$$

Parameters are the enthalpy (ΔH_m) and entropy (ΔS_m) of any unfolding transition (local or global) referenced here to its midpoint melting temperature (Tm), and ΔC_p is the difference in partial specific heat between the native and unfolded forms. The parameter ΔC_p, which determines the curvature of the plot of ΔG vs. T, is connected to the hydrophobic contribution to protein stability and in general to the change in solvent-accessible hydrophobic surface in the transition.[4] In a calorimetry experiment, one attempts to evaluate these parameters (T_m, ΔH_m, ΔS_m, ΔC_p) from heat absorption measurements through the thermal transition. Eq. 11 can then be used to project the wider range of behavior indicated in Figure 2a.

HX studies as a function of temperature well below Tm might be used to map directly the behavior seen in Figure 2a. The simulated curves in Figure 2b represent hypothetical results for NHs exchang-

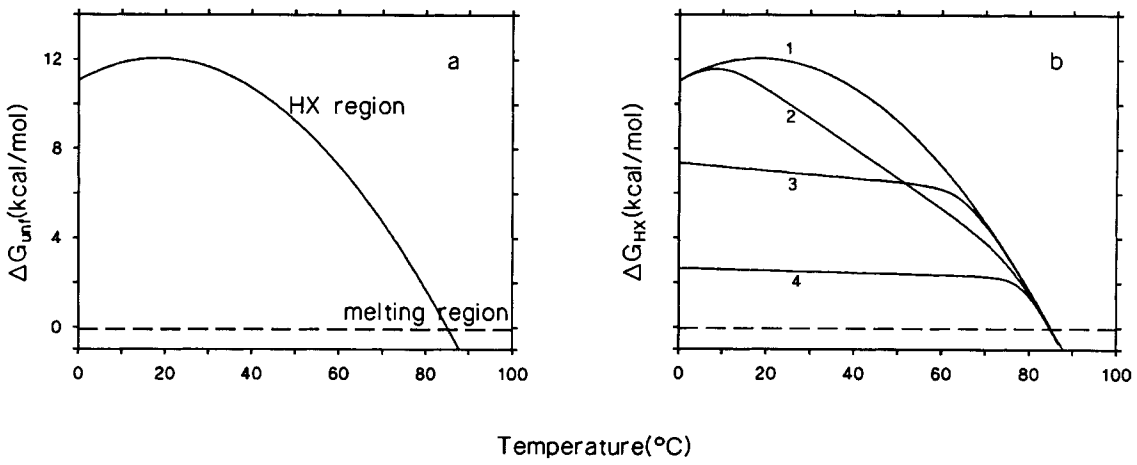

Fig. 2. Illustrative curves for the dependence of free energy on temperature. **a:** Global unfolding behavior. **b:** The same curve (1) along with faster NHs, one of which exchanges by way of a sizeable but still sub-global unfolding (2) with relatively large ΔS, and others (3 and 4) by small local unfoldings.

ing by way of both global and local fluctuations, with Eq. 7 rewritten as follows.

$$\Delta G_{HX}(T) = -RT \ln[\exp(-\Delta G(l)/RT) + \exp(-\Delta G(g)/RT)] \quad (12)$$

$\Delta G(g)$ is then expressed as in Eq. 11. To express $\Delta G(l)$, we use Eq. 11 with $\Delta C_p(l) = 0$ so that $\Delta H(l)$ and $\Delta S(l)$ become temperature independent.

The upper curve in Figure 2b simulates ΔG_{HX} values for a slowly exchanging NH that depends wholly on transient global unfolding, as in Figure 2a. NHs that exchange at faster rates because they are exposed to solvent by lower energy fluctuations produce lower lying curves. The simulated behavior shows that exchange of the faster NHs is determined by local fluctuations at lower temperatures, but at higher temperature their exchange becomes dominated by the global unfolding, just as for the denaturant simulation in Figure 1b.

The behavior seen in these simulations has been described more qualitatively before for both temperature and denaturant dependences.[9]

MATERIALS AND METHODS

Horse heart cytochrome c (type VI) and ultrapure GdmCl were from Sigma Chemical Co. Buffer solutions contained 0.1 M potassium phosphate at pD 7 in D_2O (pD values are uncorrected pH meter readings). GdmCl concentrations were measured refractometrically.[3] For the GdmCl experiments, solutions contained 0.5 M KCl to minimize possible salt-dependent effects at low GdmCl concentrations.

Cyt c was initially fully oxidized with a small amount of $K_3Fe(CN)_6$, which was removed by gel filtration.[16] The pH was set to 7, and samples were lyophilized. For H-D exchange in GdmCl, cyt c was dissolved in D_2O at 50°C (~3 mM), incubated for the experimental time period, then chilled in ice water, and reduced by adding ascorbate (10 mM). Reduction slows HX rate and enhances the nuclear magnetic resonance (NMR) resolution of the resonances studied. One-dimensional ^1H NMR spectra were then recorded, either directly or after storage on dry ice.

To measure HX time points as fast as 10 seconds at high GdmCl or high temperatures, samples were injected into a coil of 0.23 mm ID, 1.50 mm OD stainless steel tubing [high performance liquid chromatography (HPLC) tubing]. The coil was immersed in a high temperature bath (50°–70°C) for the experimental HX time and then transferred into 0°C water to halt exchange. The cyt c sample was withdrawn, reduced with ascorbate, passed through a spinning gel filtration column[16] at 5°C to remove the GdmCl and ascorbate, and analyzed by NMR as before. For faster HX rates (to <1 second), samples were exposed to the high temperature by using an HPLC pump to flow the sample through a stainless steel coil (as before) of predetermined length held at the high temperature and then directly into a cold coil to halt the exchange. Effective HX time is determined by the flow speed and hot coil volume (see also ref. 17). Subsequent processing was as described.

The one-dimensional NMR spectra used for HX measurements were acquired as 128 transients of 8,192 data points using a Bruker AM500 spectrometer. Residual solvent was suppressed by presaturation. Tyr97 to Leu98 NOE intensity was measured using cyt c at 5–10 mM with up to 25,000 scans to improve signal to noise. The overlapping Ala96 and Tyr97 peaks were saturated for 300 msec with a decoupler power of 3.8 mW. Peak areas were integrated using the program FELIX (Hare Research, Inc) with Lorenzian fitting when peaks overlapped.

The heme α-meso proton resonance in the amide region was used to normalize peak areas.

Thermal and GdmCl denaturation transitions were measured by Trp59 fluorescence on a Perkin-Elmer 650-10S spectrometer (provided by Dr. Jane Vanderkooi) or by circular dichroism using an Aviv 62DS spectropolarimeter, with oxidized cyt c at ~10 μM concentration using a fresh sample for each temperature point.

A number of tests for EX2 HX behavior were used. One test measures the intensity of an NH-NH NOE as a function of degree of H-D exchange.[17,18] To put the NOE test on a quantitative basis, a Monte Carlo simulation of exchange for two neighboring NHs was done to determine the decay of the relative NOE as HX progresses. The relative NOE may or may not decrease as HX progresses, depending on the ratio k_{cl}/k_{rc} (see Eqs. 2–4). The simulation used 30,000 molecules with two neighboring NOE-connected NHs exchanging at rates differing by a factor of 1.8, as predicted for the k_{rc} rates of Tyr97 and Leu98 NHs used here.[7] Results of the simulation are shown in Figure 8 for values of k_{cl}/k_{rc} ranging from near the EX1 limit to near the EX2 limit. The simulation program is available on request.

RESULTS

Slow HX by One-Dimensional NMR

Figure 3 shows a ^1H NMR spectrum of reduced cyt c (20°C, pD 7). A number of slowly exchanging peptide group NH hydrogens can be resolved and the fraction of each not yet exchanged can be accurately quantified. To measure exchange, samples of oxidized cyt c were held at the experimental condition in D_2O for increasing time periods and then returned to the standard condition shown, and an NMR spectrum was recorded. HX data obtained in this way for Leu98 as a function of GdmCl concentration (50°C, pD 7, D_2O) are shown in Figure 4. From these rates, the free energy for the opening reaction that governs Leu98 exchange at each GdmCl concentration (ΔG_{HX}) can be obtained (Eq. 5). The same spectra provide H-D exchange rates of all the resolved NHs and the free energy of the unfolding reaction that governs each one.

Denaturant Dependence

Figure 5a plots ΔG_{HX} values obtained in this way for the most slowly exchanging NHs in oxidized cyt c (Ala96, Tyr97, Leu98). Figure 5a also includes data through the global unfolding transition measured by fluorescence in GdmCl denaturation experiments (50°C, pD 7, D_2O). The ΔG_{HX} curve for the slowest exchanging NHs merges smoothly with the global denaturation data, and indicates a ΔG_{unf} of 9.3 kcal/mol at zero GdmCl. Available ΔG_{unf} values for cyt c from horse and cow, although measured under different conditions, are generally consistent with these results.[4,19,20] These observations indicate

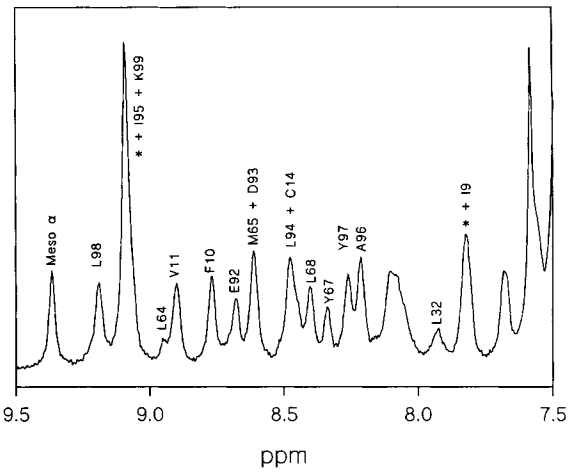

Fig. 3. Proton NMR spectrum of reduced cyt c at conditions used for the present analyses (pD 6.8, 20°C).

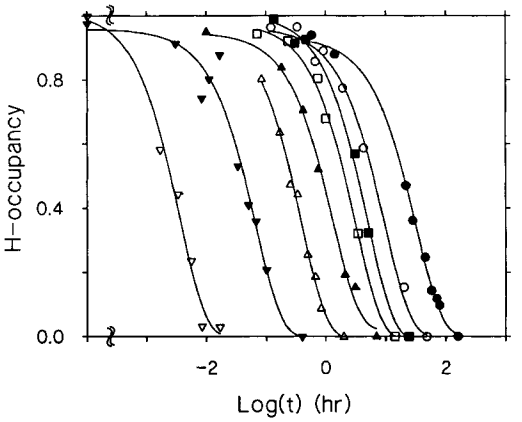

Fig. 4. Kinetic H-D exchange results for Leu98NH in oxidized cyt c at various GdmCl concentrations (50°C, pD 7). Peak areas were normalized to the α-meso heme proton (see Fig. 3). GdmCl concentrations (right to left) range from 0.0 M to 1.03 M (as plotted in Fig. 5).

that the slowest NHs do exchange by way of transient global unfolding and tend to validate the overall approach. Figure 5a also shows that ΔG_{HX} values at low GdmCl concentrations tend to rise above the linearly extrapolated denaturation data.

Figure 5b expands the low denaturant range and includes data for some faster exchanging NHs. The faster NHs exhibit a much smaller dependence on denaturant at low GdmCl concentration, with values for m close to zero. Clearly, these NHs exchange by virtue of limited fluctuations that expose little new surface area. As GdmCl concentration increases, the global unfolding HX pathway increases, overtakes the local rate, and comes to dominate the HX behavior of the faster NHs also, just as seen in the simulation described before (Fig. 1b). The difference between the best fit global curves for Ala96 and

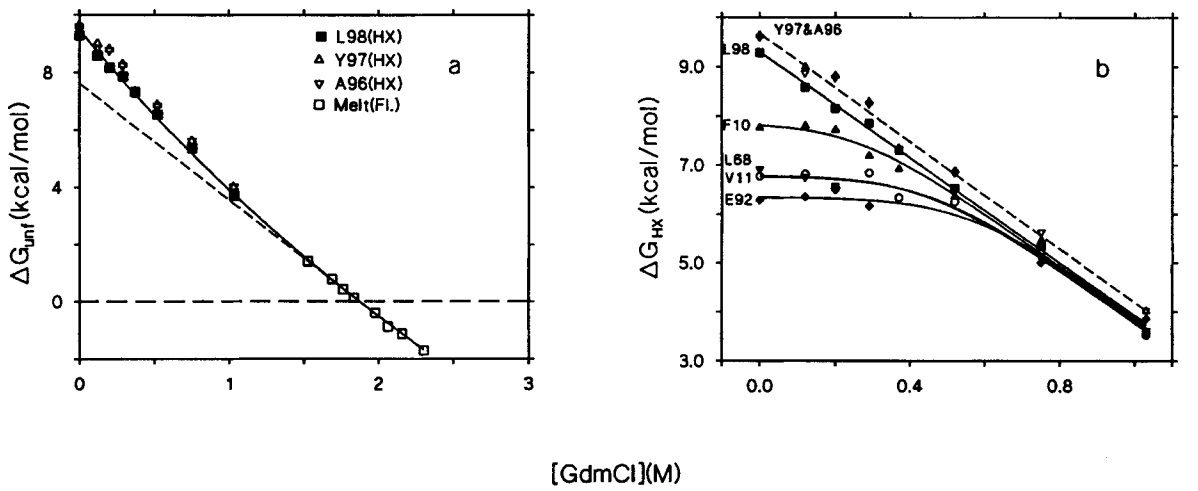

Fig. 5. HX results for slow and faster NHs as a function of denaturant concentration. **a:** ΔG values for global unfolding calculated from the slowest exchanging NHs (Eq. 5) and from denaturation data measured through the GdmCl transition by fluorescence (□). The dashed curve is the linear extrapolation to zero GdmCl from the denaturation data. **b:** The same HX results for the slowest NHs and also results from some faster NHs. The faster NHs are controlled by local fluctuations at low GdmCl and are overtaken by global unfolding at higher GdmCl. Ala96 and Tyr97 may exhibit some residual slowing in the globally unfolded form (1.6-fold slowing ~0.3 kcal).

Tyr97 and for the other NHs measured may indicate a small contribution of HX blocking in the unfolded state, with B(g) ~0.6 (defined above), so these NHs appear slowed by 1.6-fold.

These results indicate a ΔG_{unf} value of 9.3 kcal mol^{-1} for cyt c unfolding at zero GdmCl, an m value for GdmCl-induced unfolding (Eq. 8) of 5 kcal mol^{-1} M^{-1} at low GdmCl concentration, somewhat higher than the 4 kcal found through the denaturation region, and values of 33 apparent sites for Δn and 0.3 M^{-1} for K_b in the denaturant binding model (Eq. 9) (at 50°C, pD 7 in D_2O with 0.1 M potassium phosphate). (The ΔG_{unf} value obtained in a melting experiment will be lower by 0.5 kcal mol^{-1}, due to the proline effect described below.)

Temperature Dependence

Analogous behavior is seen when HX rates are measured as a function of temperature, shown for the slowest NHs (residues 96–98) in Figure 6 (pD = 7, 0.1 M phosphate buffer). The data points near the T_m (87°C) show thermal melting measured by circular dichroism at very low cyt c concentration with minimal thermal exposure so that denaturation is reversible. The ΔG_{HX} values obtained from HX data well below the melting transition (40°–70°C) for the most slowly exchanging NHs merge smoothly with the ΔG_{unf} values obtained by standard methods through the thermal transition, just as seen before for denaturant-induced unfolding. This agreement tends to validate the ΔG_{HX} measurement.

The data in Figure 6 do not determine the ΔC_p parameter well. Calorimetric determinations found

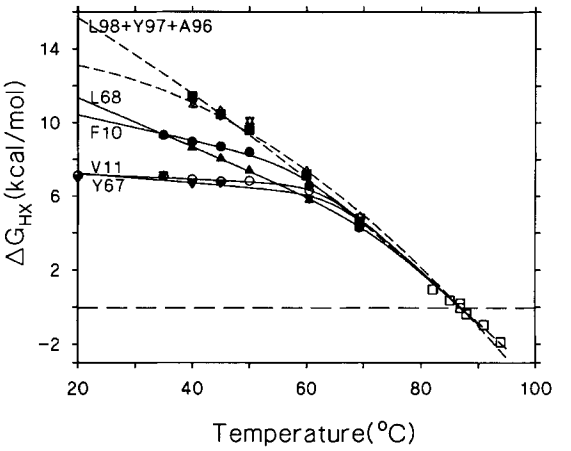

Fig. 6. HX results for the slow NHs and some faster NHs as a function of temperature. Data points above 80°C are from CD measurements through the thermal melting transition. The upper curves (dashed) are drawn using Eqs. 11 and 12 with the following parameters for global unfolding: T_m = 87°C, ΔH_m = 100 kcal mol^{-1}, ΔS_m = 277 cal mol^{-1} K^{-1}. The two dashed curves used $\Delta C_p(g)$ of 1.3[21,22] and the best fit value of 0,4 respectively. The faster protons were fit using $\Delta C_p(1) = 0$.

1.2 kcal mol^{-1} K^{-1},[21] and 1.4 kcal mol^{-1} K^{-1},[22] albeit at much lower pH. The two upper curves in Figure 6 show that the data can be well fit by a range of ΔC_p values (0.4 and 1.3 used; data fit using Eqs. 11 and 12). HX rates at the lower temperatures necessary to more accurately determine ΔC_p become prohibitively slow at the pD 7 used, but might be measured at higher pH or, with more effort, from extrapolation of denaturant curves, as in Figure 5.

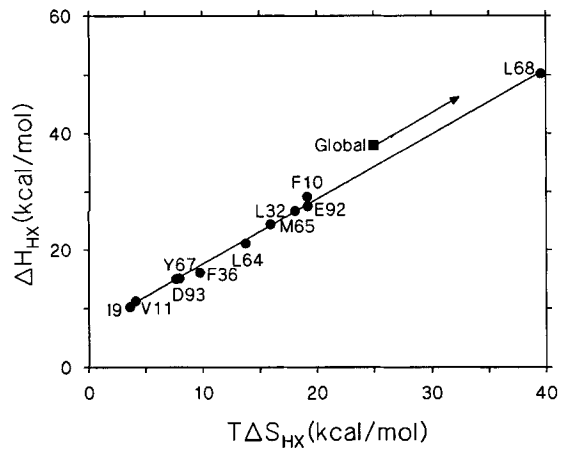

Fig. 7. Enthalpy-entropy compensation plot for the values obtained by HX, extrapolated to 25°C. The symbol marked "global" indicates the global values extrapolated to 25°C by use of a $\Delta C_p(g)$ of 1.3. For $\Delta C_p(g)$ = 0.4 kcal mol^{-1} K^{-1} (the best fit value for our data), the global value is offscale, as suggested by the arrow.

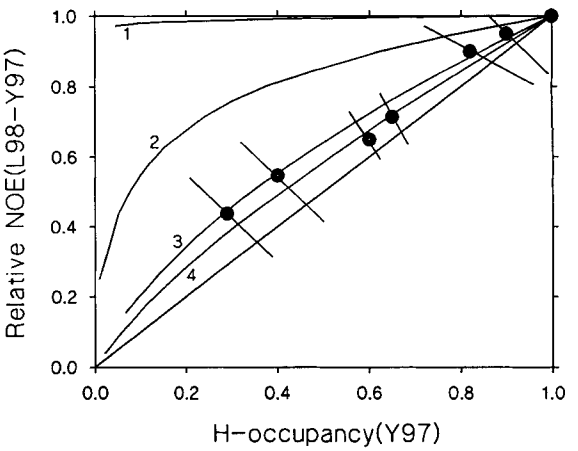

Fig. 8. The relative NOE (NOE with exchange/NOE without exchange) as a function of degree of H-exchange for two neighboring NHs. The theoretical curves shown are from simulations described in Materials and Methods. The relative NOE remains at unity for pure EX1 behavior and follows a diagonal line for EX2 behavior. The curves drawn indicate behavior expected for k_{cl}/k_{rc} values as follows: 1) 0.1; 2) 1.0; 3) 5.0; 4) 10.0. Error bars indicate the data uncertainty level on both axes.

The faster NHs shown in Figure 6 and other NHs measured (omitted here for clarity; see Fig. 7) exchange in the lower temperature range by way of smaller fluctuations with small ΔC_p. These data measure the thermodynamic parameters of the small fluctuations that govern the exchange of each faster NH. As temperature increases, the global unfolding pathway is selectively promoted and comes to dominate the exchange of these faster NHs, just as seen in the simulation of Figure 2b.

Global unfolding parameters obtained from the H-D exchange of Ala96, Tyr97, and Leu98 at pD 7 in D_2O with 0.1 M phosphate are: T_m = 87°C, ΔH_m = 100 kcal mol^{-1}, ΔS_m = 280 cal mol^{-1} K^{-1}. The best fit global ΔC_p of 0.4 kcal mol^{-1} K^{-1} is poorly determined but provides reliable values for ΔG_{unf} down to 40°C (see Fig. 6). Results for the faster NHs measured are shown in the form of an enthalpy-entropy compensation plot in Figure 7, extrapolated to 25°C.

EX2 Behavior

The analysis used here to calculate unfolding free energies assumes EX2 behavior (Eq. 4). A number of observations validate this assumption.

In a test for EX2 behavior at 50°C, the HX rate for residues 96–98 measured at pD 8.3 was found to be 20-fold faster than at the pD 7 used here. This matches the behavior expected for H-exchange in the EX2 limit, as in Eq. 4, since the chemical exchange rate, k_{rc}, is catalyzed by OH^--ion. In the EX1 case, k_{ex} would depend only on k_{op} (Eq. 3), which is likely to be essentially independent of pH in the neutral pH range. Again, the m value found, which depends on the unfolding equilibrium constant in the EX2 limit, is close to, even somewhat higher than, that seen in a GdmCl denaturation experiment. In the EX1 limit, where k_{ex} depends on the unfolding transition state, the m value found would be much smaller.

In another test, the decrease in the NOE between Leu98 and Tyr97 was measured as H-D exchange progressed (50°C, pD7) (see also refs. 17 and 18). The NHs of the neighboring helical residues exhibit similar HX slowing factors, evidently determined by the same opening reaction. In the EX1 limit, the H to D exchange of both Tyr97 and Leu98 in any given molecule will occur together upon structural opening, the NOE will decline in direct ratio to the NHs themselves, and the relative NOE—(NOE with exchange)/(NOE without exchange)—will remain constant at unity in Figure 8. In the EX2 limit, the exchange of the two NHs in a given molecule are uncorrelated so that the relative NOE decreases linearly with proton occupancy as H-D exchange progresses, as indicated by the diagonal line in Figure 8. The other curves shown in Figure 8 represent intermediate cases with different ratios of k_{cl}/k_{rc}. These curves were obtained from a Monte Carlo simulation as described in the Methods section. The data points in Figure 8, obtained from NOE measurements as exchange progressed, indicate that the exchange reaction is dominated by EX2 behavior. Thus structural reclosing (k_{cl}) is faster than k_{rc} for these NHs under the conditions tested ($k_{rc} \sim 20\ s^{-1}$).

It can be noted that as HX rates diverge from pure EX2 behavior, ΔG_{HX} values do not deviate rapidly from true ΔG_{unf} values. Even when k_{cl}/k_{rc} = 1, K_{op} measured will be half of the true K_{op} (Eqs. 2 and 4), and the error in ΔG will be only 0.4 kcal/mol (Eq. 5).

DISCUSSION

In a stable protein, local and global unfolding occur concurrently and independently. Increasing denaturant or temperature selectively promotes the global unfolding reaction because global unfolding exposes more surface and has higher chain entropy and enthalpy (at high temperatures) than local unfolding reactions. The rise of global unfolding progressively overtakes the more limited fluctuations, and this progression leads ultimately to the well-known two-state denaturation transition. The present work shows that hydrogen exchange measurements can access this behavior in a quantitative way. From this, equilibrium and kinetic information on protein unfolding and refolding may be obtained.

Earlier Work

The idea that some hydrogens may exchange by way of a global unfolding reaction has been present through much of the history of hydrogen exchange research. This was clearly stated in early tritium exchange work with carbonic anhydrase[23] and ribonuclease.[24,25] Even earlier, a dependence of DNA hydrogen exchange on global thermal unfolding was shown[26] as temperature approached the thermal transition. Subsequent work with various proteins has provided HX results that correlate in one way or another with global unfolding.[27–34] This sizeable literature is generally consistent with the conclusion that some of the slowest hydrogens in many proteins exchange by way of the transient global unfolding reaction.

HX and Global Unfolding

This paper analyzes in some depth the behavior of the slowest exchanging NHs in oxidized cyt c as well as some faster NHs. The necessary theoretical background is described (Eqs. 1–12), and HX experiments using denaturant and temperature were designed to distinguish local and global unfolding behavior.

Results obtained for oxidized cyt c show that the faster exchanging NHs are insensitive to added denaturant at low denaturant concentrations, and many are insensitive to increasing temperature, as can be expected for local unfolding reactions. The exchange behavior of the slowest NHs appears to be determined by a much larger scale unfolding reaction. When GdmCl concentration is progressively increased, the large scale unfolding is promoted, and its free energy, calculated from HX of the slowest NHs, smoothly approaches the unfolding free energy measured through the denaturant unfolding transition by standard methods (Fig. 5a). HX measured as a function of temperature similarly connects the large-scale HX unfolding with the thermal unfolding reaction (Fig. 6).

When exchange of the slowest NHs is controlled by global unfolding, K_{op} for HX (Eq. 4) becomes equal to K_{unf}, the equilibrium constant for global unfolding, and ΔG_{HX} is equal to ΔG_{unf}. Thus measured HX rates can be used to obtain the unfolding free energy, its enthalpic and entropic components, and its dependence on denaturants and other factors. This is the major result of this paper.

A secondary result relates to the analysis of protein global unfolding behavior. At low GdmCl concentrations, the curve for ΔG_{HX} against GdmCl rises above the curve obtained by linear extrapolation from GdmCl melting experiments. This behavior is consistent with some role for a site-binding model.[35]

Comparison of ΔG_{HX} and ΔG_{unf}

Several factors can make the ΔG_{HX} for unfolding differ from the value for ΔG_{unf}, even when ΔG_{unf} data are properly extrapolated to the mild conditions of the HX experiment.

Most obviously, one must consider whether the slowest exchanging NHs are in fact controlled by the global unfolding reaction. The high quality of the RNase data described below[5] provides a good example (see Cys58 in Fig. 9b). In general, HX determined by a non-global unfolding can be distinguished by a decreasing slope in the curve of ΔG_{HX} vs. denaturant as denaturant approaches zero concentration (small m value as in Fig. 1b), or by a relatively linear behavior in the temperature curve (small value for ΔC_p as in Fig. 2b).

Recent work indicating that denatured proteins may not be fully random[36] suggests a source for real differences between ΔG_{HX} and ΔG_{unf}. If residual structure modifies the free energy level of the unfolded state, this can show up in both ΔG_{HX} and ΔG_{unf}. If HX is not blocked by the residual structure (e.g., side chain but not main chain interactions occur), it is likely that ΔG_{HX}, measured at mild conditions, will appear lower than ΔG_{unf}, measured under more severe conditions through the transition. On the other hand, if HX of some NHs is blocked in the unfolded state that is accessed in denaturation experiments, then the ΔG_{HX} value obtained from these NHs will refer to some higher energy unfolded state in which their HX is allowed. The latter effect is formally encoded in the B factor noted in the theory section (see also Fig. 2b). To be effective, the residual structure must have energetically significant stability. For example, residual structure that is present only a small fraction of the time will not alter HX rates significantly, even though the transient structure can produce nuclear Overhouser effects in NMR experiments.[37–39]

The use of H_2O in denaturation experiments and D_2O in the comparative HX experiments can lead to a discrepancy, since proteins generally appear more stable in D_2O. For example, the Tm is higher in D_2O than in H_2O by 4°C for RNase[40] and for oxidized cyt c. GdmCl denaturation results for cyt c at 50°C in-

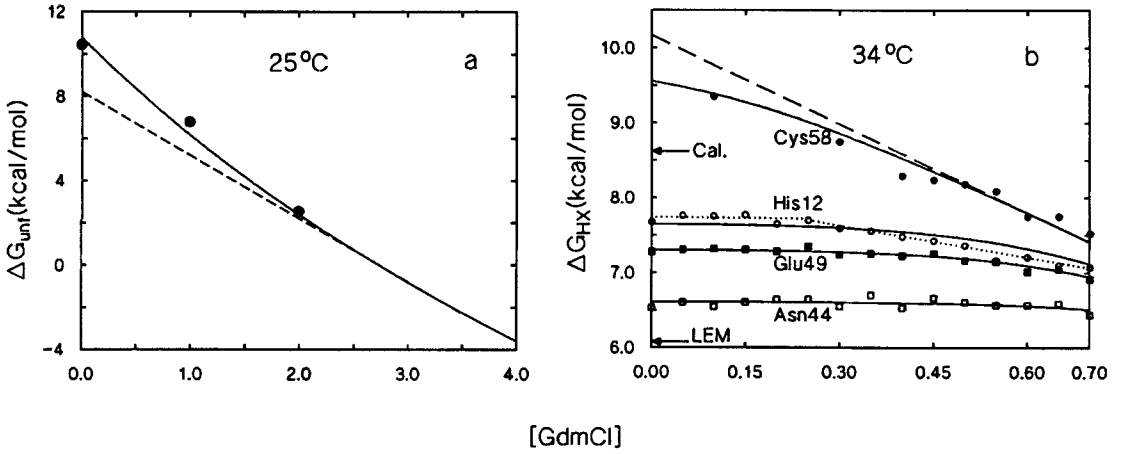

Fig. 9. Stability results for RNase at pH and pD 5.5 **a:** Linear extrapolation (—) from GdmCl denaturation data[43] and data points (•) from calorimetric results[15] in GdmCl extrapolated to 25°C. **b:** The arrows indicate ΔG_{unf} values of 6.0 kcal mol^{-1} (LEM) obtained from GdmCl denaturation results by the linear extrapolation method[5] and 8.6 kcal mol^{-1} from extrapolation of calorimetric data[15] to 34°C (in H_2O). The H-D exchange data points[5] are fit by solid curves according to Eq. 12. The dotted line through the His12 data illustrates the fitting procedure used by Mayo and Baldwin.[5]

dicate an H_2O:D_2O difference in ΔG_{unf} of 0.4 kcal mol^{-1} (not shown). Given the curvature of the temperature curve (Fig. 2a), the difference at lower temperature is likely to be even smaller.

The slow cis-trans isomerization of the prolyl peptide bond will lead to a discrepancy between ΔG_{HX} and ΔG_{unf}. In an equilibrium melting experiment, the proline residues in the unfolded state have time to reach their isomeric equilibrium distribution, but this is not true for the unfolded molecules in the HX experiment. For example, in the present HX experiments (pD 7, 50°C, $k_{rc} \sim 100\ s^{-1}$), cyt c must spend only 50 msec in the transient globally unfolded state in order to exchange its slowest NHs (even though the HX experiment consumes 2 weeks of real time). Proline isomerization requires a much longer time period (minutes[41]). Thus the unfolded state probed by the HX experiment occupies a higher free energy level than the equilibrium unfolded state, because it does not have time to relax to the lower free energy state with the prolines at their cis-trans equilibrium values. This discrepancy in free energy arises because the total population of transiently unfolded molecules that exists at any instant (with prolines in their proper equilibrium isomeric distribution) is larger than the population that contributes to hydrogen exchange (with prolines only in their native isomeric positions).

The proline-dependent free energy increment can be calculated as follows.

$$\Delta\Delta G_{exp} = \Delta G_{HX} - \Delta G_{unf} = RT \ln (1 + K) \quad (13)$$

Here K is the isomerization constant in the equilibrium unfolded state, written in the direction for which K = 0 in the native state. This equation can be derived from a pertinent thermodynamic cycle (see also ref. 42).

In native cyt c, all four prolines are trans. If it is assumed that each proline position attains a cis/trans ratio of 1/4 in the equilibrium unfolded state (K = 0.25), then each contributes RT ln (1 + 0.25), for a total discrepancy of 0.54 kcal (at 30°C). When a proline is cis in the native protein, the differential is larger, given by RT ln (1 + 4) ≈ 1 kcal/proline.

An altered isomeric ratio in the unfolded state will modify the calculation. Adler and Scheraga[43] report that the two prolines that are cis in native RNase A exhibit an equilibrium constant in the unfolded state (trans/cis) of about 1.6. Thus these two prolines contribute 2 × RT ln (1 + 1.6) = 1.16 kcal, and together with the two trans prolines lead to a proline-dependent free energy differential (ΔG_{HX} − ΔG_{unf}) in unfolded RNase of 1.4 kcal (at 34°C).

In summary, the value of ΔG_{HX}, the free energy for global unfolding measured by HX, can be larger than the ΔG_{unf} value determined by melting experiments due especially to the proline effect, and possibly also due to the use of D_2O and H_2O in the different experiments and to residual HX blocking in the unfolded state that is accessed by melting. Factors that may make ΔG_{HX} values appear low include the spurious use of slow NHs that do not depend fully on global unfolding and the presence of increased residual structure in the unfolded state at mild HX conditions (with the probe NHs not blocked).

Ribonuclease A

Available HX and melting data for RNase enlarge this view. Figure 9a and 9b compares calorimetric,[15]

linear extrapolation,[44] and HX[5] results, all at pH or pD 5.5.

Figure 9a shows the linear extrapolation curve dictated by GdmCl denaturation data[43] (pH 5.5, 25°C). The data points, from calorimetric melting experiments in GdmCl extrapolated to 25°C,[15] rise above the linear extrapolation curve at low GdmCl. Similarly, the arrows in Figure 9b (34°C, pH 5.5) point to ΔG_{unf} values of 6.0 kcal mol^{-1} from linear extrapolation of GdmCl denaturation results[5] and 8.6 kcal mol^{-1} from extrapolation of published calorimetric data.[15] These results show that linear extrapolation fron RNase melting data point to unfolding free energies at zero GdmCl that are lower than extrapolated calorimetric values (by 2.2 kcal mol^{-1} at 25°C in Fig. 9a and by 2.6 kcal mol^{-1} at 34°C in Fig. 9b). This behavior is like that seen for cyt c in Figure 5a, in which ΔG_{unf} was determined directly at low GdmCl from HX experiments.

Figure 9b treats published HX results for RNase[5] (34°C, pD 5.5; recalculated according to ref. 7). Mayo and Baldwin[5] fit their HX data (Fig. 9b) by one or two straight lines, as shown for His12 (dotted line), and noted a relationship between the slope (m value) for each NH and its ΔG_{HX} value. We fit the data according to Eq. 12 (solid lines), based on local and global unfolding. The RNase behavior appears similar to that found for cyt c, with the HX of one residue, Cys58, near the global unfolding limit. The upper dashed line through the Cys58 data is drawn with a slope (m value) of 4 kcal mol^{-1} M^{-1}, taken from the calorimetric results in Figure 9a at a similar denaturant level. This use of the global m value helps to identify authentic global unfolding behavior, and points to ΔG_{HX} of 10.15 kcal. Alternatively, Mayo and Baldwin drew a straight line directly through the Cys58 data points, with a slope of 3 kcal mol^{-1} M^{-1}, equal to that for the linear extrapolation curve in Figure 9a. This points to ΔG_{HX} of 9.6 kcal. These differences produce only a small uncertainty in ΔG_{HX}, between 9.6 and 10.1 kcal mol^{-1}. In either case, however, these ΔG_{HX} values are considerably higher than the ΔG_{unf} value obtained from denaturation results (6.0 or 8.6 kcal mol^{-1}).

The interpretation of the RNase data suggested by Mayo and Baldwin[5] stemmed from the apparent 3.6 kcal discrepancy between 9.6 kcal for ΔG_{HX} indicated by Cys58 and the 6.0 kcal ΔG_{unf} found by linear extrapolation of melting data (see Fig. 9b). The considerations described here suggest that one should more properly compare the 10.15 kcal obtained from the global part of the Cys58 HX curve and the 8.6 kcal value from calorimetric melting results. The differential, 1.55 kcal, appears to represent essentially the expected proline effect, computed above at 1.4 kcal.

In summary, available HX data for RNase as a function of GdmCl concentration support the result seen for cyt c. ΔG_{HX} obtained from a very slowly exchanging NH in RNase provides an accurate measurement for ΔG_{unf} when corrected for the expected proline effect.

On protein refolding

It is noteworthy that results obtained here demonstrate EX2 behavior for exchange of the hydrogens controlled by global unfolding. This requires that the refolding of cyt c from the globally unfolded state (k_{cl}) proceeds more rapidly than the chemical HX rate (k_{rc}) at a number of solution conditions (0–1 M GdmCl at 50°C in Fig. 5; 40°–70°C in no GdmCl in Fig. 6; all at pD 7). The k_{rc} rate for HX under these conditions extends up to 80 s^{-1}. The ability of cyt c and other proteins to fold rapidly has been considered in more detail in kinetic folding experiments.[45] The present, direct HX experiments access folding kinetics but are unlike typical kinetic folding experiments in some ways. The protein is not exposed to gross unfolding conditions for lengthy time periods. Intermediate states in unfolding and refolding are populated on the basis of their equilibrium free energy level at native conditions and are not dependent on the size of kinetic folding barriers.

ACKNOWLEDGMENTS

This work was supported by NIH research grant DK11295. We thank Jane Vanderkooi for use of the fluorescence spectrometer, Eleanor Brown for access to a CD spectrometer, Tobin Sosnick for helpful discussions, H. Roder for assistance in the early temperature experiments, and R.L. Baldwin for comments on the manuscript. We thank H. Qian, S.L. Mayo, and A. Morton for sending a preprint of their manuscript on similar issues.

REFERENCES

1. Nozaki, Y., Tanford, C. The solubility of amino acids, diglycine, and triglycine in aqueous guanidine hydrochloride solutions. J. Biol. Chem. 245:1648–1652, 1970.
2. Aune, K.C., Tanford, C. Thermodynamics of the denaturation of lysozyme by guanidine hydrochloride. II. Dependence on denaturant concentration at 25°C. Biochemistry 8:4586–4590, 1969.
3. Pace, C.N. Determination and analysis of urea and guanidine hydrochloride denaturation curves. Methods Enzymol. 131:266–280, 1986.
4. Privalov, P.L., Khechinashvili, N.N. A thermodynamic approach to the problem of stabilization of globular protein structure: A calorimetric study. J. Mol. Biol. 86:665–684, 1974.
5. Mayo, S.L., Baldwin, R.L. Guanidinium chloride induction of partial unfolding in amide proton exchange in RNase A. Science 262:873–876, 1993.
6. Hvidt, A., Nielsen, S.O. Hydrogen exchange in proteins. Adv. Protein Chem. 21:287–386, 1966.
7. Bai, Y., Milne, J.S., Mayne, L., Englander, S.W. Primary structure effects on peptide group hydrogen exchange. Proteins 17:75–86, 1993.
8. Connelly, G.P., Bai, Y., Jeng, M.-F., Englander, S.W. Isotope effect in peptide group hydrogen exchange. Proteins: 17:87–92, 1993.
9. Englander, S.W., Kallenbach, N.R. Hydrogen exchange and structural dynamics of proteins and nucleic acids. Q. Rev. Biophys. 16:521–655, 1984.
10. Linderstøm-Lang, K.U. Deuterium exchange between pep-

tides and water. In: "Symposium on Peptide Chemistry." Chem. Soc. Spec. Publ. 2:1–20, 1955.
11. Englander, S.W. Measurement of structural and free energy changes in hemoglobin by hydrogen exchange methods. Ann. N.Y. Acad. Sci. 244:10–27, 1975.
12. Englander, S.W., Englander, J.J., McKinnie, R.E., Ackers, G.K., Turner, G.J., Westrick, J.A., Gill, S.J. Hydrogen exchange measurement of the free energy of structural and allosteric change in hemoglobin. Science 256:1684–1687, 1992.
13. Woodward, C.K., Simon, I., Tuchsen, E. Hydrogen exchange and the dynamic structure of proteins. Mol. Cell. Biochem. 48:135–160, 1982.
14. Santoro, M.M., Bolen, D.W. A test of the linear extrapolation of unfolding free energy changes over an extended denaturant concentration range. Biochemistry 31:4901–4907, 1992.
15. Makhatadze, G.I., Privalov, P.L. Protein interaction with urea and guanidium chloride: A calorimetric study. J. Mol. Biol. 226:491–505, 1992.
16. Jeng, M.F., Englander, S.W. Stable submolecular folding units in a non-compact form of cytochrome c. J. Mol. Biol. 221:1045–1063, 1992.
17. Roder, H., Wagner, G., Wüthrich, K. Amide proton exchange in proteins by EX1 kinetics: Studies of the basic pancreatic trypsin inhibitor at variable pD and temperature. Biochemistry 24:7396–7407, 1985.
18. Wagner, G. A novel application of nuclear overhauser enhancement(NOE) in proteins: Analysis of correlated events in the exchange of internal labile protons. Biochem. Biophys. Res. Commun. 97:614–620, 1980.
19. Knapp, J.A., Pace, C.N. Guanidine hydrochloride and acid denaturation of horse, cow, and *Candida krusei* cytochromes c. Biochemistry 13:1289–1294, 1974.
20. Tsong, T.Y. Ferricytochrome c chain folding measured by the energy transfer of tryptophan 59 to the heme group. Biochemistry 15:5467–5473, 1976.
21. Potekhin, S., Pfeil, W. Microcalorimetric studies of conformational transitions of ferricytochrome c in acidic solution. Biophys. Chem. 34:55–62, 1989.
22. Kuroda, Y., Kidokoro, S., Wada, A. Thermodynamic characterization of cytochrome c at low pH. Observation of the molten globule state and of the cold denaturation process. J. Mol. Biol. 223:1139–1153, 1992.
23. Rosenberg, A., Chakravarti, K. Studies of hydrogen exchange in proteins. J. Biol. Chem. 243:5193–5201, 1968.
24. Woodward, C.K., Rosenberg, A. Studies of hydrogen exchange in proteins. V. The correlation of ribonuclease exchange kinetics with the temperature-induced transition. J. Biol. Chem. 246:4105–4113, 1971.
25. Woodward, C.K., Rosenberg, A. Studies of hydrogen exchange in proteins. VI. Urea effects on ribonuclease kinetics leading to a general model for hydrogen exchange from folded proteins. J. Biol. Chem. 246:4114–4121, 1971.
26. Printz, M.P., von Hippel, P.H. Hydrogen exchange studies of DNA structure. Proc. Natl. Acad. Sci. USA 53:363–370, 1965.
27. Wagner, G., Wüthrich, K. Structural interpretation of amide proton exchange in basic pancreatic trypsin inhibitor and related proteins. J. Mol. Biol. 134:75–94, 1971.
28. Roder, H. Structural characterization of protein folding intermediates by proton magnetic resonance and hydrogen exchange. Methods Enzymol. 176:446–473, 1989.
29. Wedin, R.E., Delepierre, M., Dobson, C.M., Poulsen, F.M. Mechanisms of hydrogen exchange in proteins from nuclear magnetic resonance studies of individual tryptophan indole NH hydrogens in lysozyme. Biochemistry 27:1098–1103, 1982.
30. Delepierre, M., Dobson, C.M., Selvarajah, S., Poulsen, F.M. Correlation of hydrogen exchange behavior and thermal stability of lysozyme. Biochemistry 21:1098–1103, 1982.
31. Gooley, P.R., Zhou, D., Mackenzie, E.N. Comparison of amide proton exchange in reduced and oxidized *Rhodobacter capsulatus* cytochrome c: A ^{1}H-^{15}N NMR study. J. Biomol. NMR 1:145–154, 1991.
32. Kim, K., Woodward, C. Protein internal flexibility and global stability: Effect of urea on hydrogen exchange rates of bovine pancreatic trypsin inhibitor. Biochemistry 32: 9609–9613, 1993.
33. Loh, S.N., Prehoda, K.E., Wang, J., Markley, J.L. Hydrogen exchange in unligated and ligated staphylococcal nuclease. Biochemistry 32:11022–11028, 1993.
34. Clarke, J., Hounslow, A.M., Bycroft, M., Fersht, A.R. Local breathing and global unfolding in hydrogen exchange of barnase and its relationship to protein folding pathways. Proc. Natl. Acad. Sci. USA. 90:9837–9841, 1993.
35. Schellman, J.A. The thermodynamic stability of proteins. Annu. Rev. Biophys. Biophys. Chem. 16:115–137, 1987.
36. Dill, K.A., Shortle, D. Denatured states of proteins. Annu. Rev. Biochem. 60:795–825, 1991.
37. Wüthrich, K. NMR assignments as a basis for structural characterization of denatured states of globular proteins. Curr. Opin. Struc. Biol. 4:93–99, 1994.
38. Logan, T.M., Theriault, Y. and Fesik, S.W. Structural characterization of the FK506 binding protein unfolded in urea and guanidine hydrochloride. J. Mol. Biol. 236:637–648, 1994.
39. Lumb, K.J., Kim, P.S. Formation of a hydrophobic cluster in danatured bovine pancreatic trypsin inhibitor. J. Mol. Biol. 236:412–420, 1994.
40. Scheraga, H.A. Helix-random coil transformations in deuterated macromolecules. Ann. N.Y. Acad. Sci. 84:608–616, 1960.
41. Nall, B. Proline isomerization and protein folding. Comments. Mol. Cell Biophys. 3:123–143, 1985.
42. Jackson, S.E., Fersht, A.R. Folding of chymotrypsin inhibitor 2. 1. Evidence for a two-state transition. Biochemistry. 30:10428–10435.
43. Adler, M., Scheraga, H.A. Nonnative isomers of proline-93 and -114 predominate in heat-unfolded ribonuclease A. Biochemistry. 29:8211–8216, 1990.
44. Pace, N.C., Douglas, L.V., Thomson, J.A. pH dependence of the urea and guanidine hydrochloride denaturation of ribonuclease A and ribonuclease T1. Biochemistry. 29: 2564–2570, 1990.
45. Sosnick, T., Mayne, L., Hiller, R., Englander, S.W. The barriers in protein folding. Nature Struct. Biol. 1:149–156, 1994.